Supplemental Results and Discussion

Antigen-specific B-cell depletion for precision therapy of mucosal pemphigus vulgaris

Pharmacologic and toxicologic effects of soluble anti-DSG3 antibodies

After incubation of DSG3-CAART with physiologic (50-200 RU/mL) levels of PV IgG, PV IgG induced a titer-dependent increase in DSG3-CAART IFNγ production, with mean levels of 0.4, 0.9, 1.1, and 1.4 ng/mL at 50, 100, 150, and 200 RU/mL. Incubation of DSG3-CAART with 50 RU/mL PV IgG in the presence or absence of anti-DSG3 Nalm6 cells resulted in mean IFNγ levels of 10.5 and 0.7 ng/mL respectively, indicating that IFNγ production induced by soluble PV IgG is 15-fold lower than levels induced by target cell encounter (**Supplementary Figure 4**). T-cell activation upregulates cell-surface adhesion molecules(1). Accordingly, DSG3-CAART but not NTD T-cells demonstrated homotypic aggregation with increasing PV IgG titers. CART19 demonstrated basal aggregation in medium alone, which increased in response to PV IgG, potentially due to anti-mouse antibodies commonly present in human sera(2). Median DSG3-CAART and CART19 cluster areas were comparable, increasing from 50-150 RU/mL but decreasing at 200 RU/mL, reflecting either activation-induced cell death or further compaction of clusters, the latter favored since IFNγ levels indicate continued activation of DSG3-CAART from 50-200 RU/mL. Collectively, these and prior studies on soluble autoantibody-CAAR interactions indicate that 1) DSG3-CAART can renew free cell-surface CAAR and proliferate in response to PV IgG(3), which may increase efficacy in targeting rare DSG3-specific B-cells; 2) complement-dependent or antibody-dependent cellular cytotoxicity is less likely due to the IgG4-predominance of PV autoantibodies(4, 5); and 3) risk of cytokine release syndrome due to IFNγ production is uncertain, but mitigated by a conservative fractionated-dosing plan. Interestingly,

because Th1 insufficiency has been postulated as a pathogenic factor in pemphigus, interferon therapy has been evaluated in both pemphigus as well as the related autoimmune blistering disease bullous pemphigoid. In a randomized controlled trial of 30 patients, PV patients demonstrated elevated IL-4 and decreased IFNγ compared to healthy controls at baseline, which reversed after IFNα therapy, concomitant with improved clinical outcome(6). In an open-label trial of 9 bullous pemphigoid patients, patients treated with IFNγ demonstrated clinical improvement, along with decreased serum IL-4 and autoantibody concentrations(7). Thus, IFNγ induction resulting from DSG3-CAART activation is not expected to worsen and may improve PV pathophysiology.

We next evaluated the potential for PV IgG to redirect DSG3-CAART cytolysis toward FcγR-expressing cells. Primary human monocytes express FcγRI-III and neonatal Fc receptor, which bind monomeric IgG (**Supplementary Figure 5**). Primary human NK cells express low-affinity FcγRIII, which does not effectively affix monomeric IgG. Cytolysis of primary human monocytes or NK cells was not observed after co-incubation with DSG3-CAART and 20-150 RU/mL PV IgG relative to positive control OKT3, which activates the endogenous TCR/CD3 complex(8). Furthermore, PV IgG did not redirect lysis of K562 cells overexpressing individual FcγRs (**Supplementary Figure 6A,B**). IFNγ was elevated in all DSG3-CAART co-cultures with PV IgG/OKT3, even in the absence of target cells, reflecting direct antibody stimulation of IFNγ production (**Supplementary Figure 5E,6C**).

Off-target interactions of DSG3-CAART

DSG3-CAART does not demonstrate cytotoxicity toward primary human keratinocytes and human skin xenografts(3), which express the natural DSG3 ligands desmocollin (DSC) 1 and 3(9). DSG3 does not physiologically interact with DSC2 due to differing tissue expression

patterns, but DSG3-DSC2 ectodomains can interact in vitro(10). We therefore evaluated potential DSG3-CAART cytotoxicity against a panel of DSC2-expressing primary human cells. When co-cultured with anti-DSG3 PVB28 cells, DSG3-CAART produced cytotoxic T-cell cytokines TNFα and IFNγ, whereas low to undetectable levels were observed after DSG3-CAART co-culture with other primary human cells (**Supplementary Figure 7A,B**). CXCL9-10, IL-12, and EGF were relatively increased in some epithelia, which is of unclear significance but might be attributable to basal CAAR signaling(11) amplified by allogeneic stimulation. Furthermore, DSG3-CAART did not demonstrate evidence of cytotoxicity against most desmosome-expressing cells, except for 30% greater change in cellular impedance than NTD T-cells against renal cortical and colonic epithelial cells at a 50:1 effector-to-target ratio (**Supplementary Figure 7C**), a ratio not likely to be achieved in vivo.

We also pursued an unbiased, high-throughput approach to identify potential off-target interactions by screening a cell-based array of 5300+ membrane proteins with soluble Fc-tagged DSG3EC1-4 CAAR ectodomain. A weak interaction with a C-type lectin membrane protein, CLEC4M (isoform V8)(12), was detected at the highest (20 μg/mL) concentration relative to Fc-isotype control (**Figure 4A,B**). CLEC4M is expressed in liver, lung, and other tissues and binds to glycosylated regions of proteins, which are present in both the DSG3 CAAR and Fc domains. To assess functional relevance, we measured IFNγ production following DSG3-CAART co-culture with K562 cells expressing CLEC4M V8 or V1 full-length isoform. DSG3-CAART demonstrated IFNγ production after exposure to anti-DSG3 PVB28 cells but not K562 cells overexpressing either CLEC4M isoform (**Figure 4C**). Additionally, we assessed primary human cells reported to naturally express CLEC4M(13-15); qPCR only verified pulmonary microvascular endothelial expression (**Figure 4D-F**). IFNγ and TNFα were not detected in

DSG3-CAART co-culture supernatants. Higher levels of CXCL8-10 and MCP-1 were detected in pulmonary microvascular endothelial cell co-cultures with DSG3-CAART. However, DSG3-CAART did not induce cytolysis of pulmonary endothelial cells and induced changes in hepatic endothelial cell impedance only at a 50:1 effector-to-target ratio. Collectively these data suggest that CLEC4M binding in the membrane proteome array may have been an artifact of additional or aberrant glycosylation sites in the Fc-tagged DSG3EC1-4 protein that are not present in DSG3-CAART, or that DSG3-CAART interaction with CLEC4M-expressing cells does not promote effective immunologic synapse formation.

Collectively, the data from mouse toxicology experiments, including human skin xenografts, together with broad screens against panels of primary human cells and membrane proteome arrays, do not identify productive off-target interactions of DSG3-CAART.

1. Zumwalde NA, Domae E, Mescher MF, and Shimizu Y. ICAM-1-dependent homotypic aggregates regulate CD8 T cell effector function and differentiation during T cell activation. *J Immunol.* 2013;191(7):3681-93.
2. Klee GG. Human anti-mouse antibodies. *Arch Pathol Lab Med.* 2000;124(6):921-3.
3. Ellebrecht CT, Bhoj VG, Nace A, Choi EJ, Mao X, Cho MJ, Di Zenzo G, Lanzavecchia A, Seykora JT, Cotsarelis G, et al. Reengineering chimeric antigen receptor T cells for targeted therapy of autoimmune disease. *Science.* 2016;353(6295):179-84.
4. Funakoshi T, Lunardon L, Ellebrecht CT, Nagler AR, O'Leary CE, and Payne AS. Enrichment of total serum IgG4 in patients with pemphigus. *Br J Dermatol.* 2012;167(6):1245-53.
5. Futei Y, Amagai M, Ishii K, Kuroda-Kinoshita K, Ohya K, and Nishikawa T. Predominant IgG4 subclass in autoantibodies of pemphigus vulgaris and foliaceus. *Journal of Dermatological Science.* 2001;26(1):55-61.
6. El-Darouti MA, Hegazy RA, Abdel Hay RM, El Hawary MS, Tawdy AM, Fawzy MM, and Rashed LA. Study of T helper 1 and T helper 2 responses in pemphigus vulgaris patients receiving interferon alpha 2a injections in addition to a standard protocol therapy: a randomized controlled trial. *Arch Dermatol Res.* 2015;307(4):299-307.
7. Nakama T, Ishii N, Ono F, Hamada T, Yasumoto S, and Hashimoto T. Efficacy of interferon-gamma in patients with refractory bullous pemphigoid. *J Dermatol.* 2007;34(11):737-45.

8. Itoh K, Balch CM, Trial J, and Platsoucas CD. CD8+ T cells lyse autologous monocytes in the presence of anti-CD3 monoclonal antibody: association with interleukin-1 production. *Cell Immunol.* 1988;114(2):257-71.
9. Getsios S, Huen AC, and Green KJ. Working out the strength and flexibility of desmosomes. *Nat Rev Mol Cell Biol.* 2004;5(4):271-81.
10. Harrison OJ, Brasch J, Lasso G, Katsamba PS, Ahlsen G, Honig B, and Shapiro L. Structural basis of adhesive binding by desmocollins and desmogleins. *Proceedings of the National Academy of Sciences.* 2016;113(26):7160-5.
11. Milone MC, Fish JD, Carpenito C, Carroll RG, Binder GK, Teachey D, Samanta M, Lakhal M, Gloss B, Danet-Desnoyers G, et al. Chimeric receptors containing CD137 signal transduction domains mediate enhanced survival of T cells and increased antileukemic efficacy in vivo. *Mol Ther.* 2009;17(8):1453-64.
12. Li H, Wang JX, Wu DD, Wang HW, Tang NL, and Zhang YP. The origin and evolution of variable number tandem repeat of CLEC4M gene in the global human population. *PLoS One.* 2012;7(1):e30268.
13. Uhlen M, Fagerberg L, Hallstrom BM, Lindskog C, Oksvold P, Mardinoglu A, Sivertsson A, Kampf C, Sjostedt E, Asplund A, et al. Proteomics. Tissue-based map of the human proteome. *Science.* 2015;347(6220):1260419.
14. https://www.proteinatlas.org/ENSG00000104938-CLEC4M.
15. GTEx Portal, accessed 07/24/19.

Methods

DSG3-CAART production. DSG3 EC1-4 CAAR construction was previously described(*8*). For lentivirus production, $8x10^6$ 293T cells were seeded in a T150 flask and transfected at 50-70% confluency with packaging plasmids pRSV-Rev and pGAG/POL, envelope plasmid Pcl vsvg (Nature Technology Corp), and pTRPE-DSG3-CAAR, complexed with Lipofectamine 2000 (Life Technologies). Supernatant was harvested after 24 and 48 hours, filtered through a 0.45 micron polyethersulfone membrane (Genesee Scientific), concentrated at 17,200xg for 24 hours at 4°C and stored at -80°C. Titer (transforming units/mL) was quantitated by transducing primary human T-cells with serial dilutions of lentivirus and evaluating DSG3-$CAAR^+$ cell percentage at limiting dilution by flow cytometry.

Primary human T-cells were stimulated with anti-CD3/CD28 beads (Dynabeads, Life Technologies) at a bead:cell ratio of 3:1 in culture media supplemented with 100 IU/mL interleukin 2 (Proleukin) for 24 hours, followed by mock or DSG3-CAAR transduction at a multiplicity of infection ≥5. Cell concentration, number, and volume were evaluated every 40-56 hours during expansion using a Multisizer 4e (Beckman Coulter) instrument. DSG3-CAAR transduction was 30% or greater for functional assays.

Human ELISpot.

Patient characteristics. Patient 1: 43 year old male, relapsed mucosal disease, DSG3 ELISA 152 U/mL; Patient 2: 42 year old female, new onset mucocutaneous disease, DSG3 ELISA 21 U/mL; Patient 3: 36 year old male, chronic active mucosal disease, DSG3 ELISA 178 U/mL. PV patients were not on systemic immunosuppressants at the time of blood draw.

Venipuncture was performed under Institutional Review Board protocols. Peripheral blood mononuclear cells (PBMCs) were isolated by Ficoll centrifugation and stored at -170°C.

ELISpot assay: DSG3-CAART, CART19, nontransduced (NTD) T cells, and PBMCs were thawed and recovered in RPMI media supplemented with 10 ng/ml recombinant human IL-2 (MabTech) for 16-24 hours. B-cells were purified from PBMCs by negative selection (EasySep Human B-cell Enrichment Kit, StemCell Technologies) and co-cultured with DSG3-CAART, CART19 or NTD cells at a 1:1 ratio for 6 hours. After 6 hours, 10 ng/ml of IL-2 (MabTech) and 1 μg/mL of R848 (MabTech) were added to the co-culture and allowed to incubate for an additional 48 hours. After 35% ethanol activation, ELISpot wells (Millipore) were incubated with 5 μg/ml of recombinant DSG3 EC1-5 extracellular domain (rhDSG3, Euroimmun), 5 μg/ml of bovine serum albumin (BSA) or 15 μg/ml of human total IgG monoclonal antibody MT91/145 (MabTech) overnight at 4°C. 100,000 B-cells were plated for anti-DSG3 IgG detection and 1,000-2,000 B cells were plated for total IgG detection. After incubation in ELISpot plates for 18 hours, cells were removed and plates washed five times with 200 μL PBS. For detection, 1 μg/ml detection antibody MT78/145 (MabTech) was added and incubated for 2 hours at room temperature. Plates were washed five times with PBS, and incubated with streptavidin-HRP (MabTech) for 1 hour at room temperature. Plates were washed, developed using TMB substrate (MabTech), and quantitated using a CTL ImmunoSpot S3 Analyzer with ImmunoSpot v5.1.36 software.

The percent of total B-cells that are IgG B-cells was calculated by averaging the IgG B-cell spot counts in PV patients (**Figure 1**, rows 1-2, middle column for each pateint) and dividing by the total number of B-cells plated per well. The percent of IgG B-cells that are DSG3-reactive was calculated by dividing the spot counts in the PV B-cells + NTD condition (**Figure 1**, row 1)

with the number of IgG B-cells plated per well (extrapolating the average number of IgG B-cells plated per well to the number of cells plated in the DSG3- versus anti-hIgG-coated wells.) The reduction in anti-DSG3 IgG B-cells was estimated by dividing the number of DSG3-specific B-cells in DSG3-CAART- or CART19- versus NTD-treated conditions (**Figure 1**, first column for each patient, rows 2-3 versus 1).

Dose-activity study using a PV polyclonal hybridoma model. All in vivo studies were performed under protocols approved by the Institutional Animal Care and Use Committee. NOD-SCID-$\gamma_c^{-/-}$ (NSG) mice were bred by the Stem Cell and Xenograft Core. Hybridomas were transduced with lentiviral vectors encoding click-beetle luciferase and green fluorescent protein (GFP) and sorted to enrich for GFP+surface IgG+ cells.

Experimental design. AK18, AK19 and AK23 hybridomas (Masayuki Amagai, Keio University, Tokyo, Japan) were mixed at equal proportions and $2x10^5$ total hybridoma cells were injected intravenously into NSG mice (age 6-8 weeks), 4 groups of 5 mice each after pre-treatment with 600 mg/kg intravenous immunoglobulin (IVIG, Privigen) daily for 2 days. After 4 days, $3x10^7$, $1x10^7$, $3x10^6$ DSG3 EC1-4 CAAR T-cells or $3x10^7$ control NTD T-cells (in a 200 µl volume) were injected intravenously. An additional 5 mice each were injected with $3x10^7$ or $1x10^7$ DSG3-CAART cells without hybridomas. Animals were monitored for toxicity as evidenced by >10% weight loss, loss of fur, diarrhea, conjunctivitis, or hind-limb paralysis and otherwise euthanized 17 days after target cell injection. For some experiments, $1x10^7$ DSG3-CAART (12 mice), a 1:1 mixture of DSG3-EC1-3 and DSG3-EC1-4 CAAR T cells (8 mice), or CART19 (12 mice) were injected intravenously. 4 mice each from the CART19 and DSG3-

CAART-treated groups were euthanized 7 days after T-cell injection with the remainder 15 days after T-cell injection for examination of time-dependent toxicologic effects.

Bioluminescence imaging. 150 mg/kg D-luciferin potassium salt (GoldBio) was injected intraperitoneally, combined with 600 mg/kg IVIG. Mice were anesthetized with 2% isoflurane, and bioluminescence was quantified with an IVIS Lumina III (PerkinElmer) in automatic exposure mode 10 minutes after luciferin injection. Total flux was quantified using Living Image 4.5 software (PerkinElmer) by drawing rectangles of identical area around mice reaching from head to 50% of the tail length; background bioluminescence was subtracted for each image individually.

Enzyme-linked immunosorbent assay (ELISA). Serum samples were processed using serum-separator tubes (BD) and stored at -80^{o}C. Anti-DSG3 antibody titers were determined by DSG3 ELISA (Euroimmun) at a serum dilution of 1:10 and goat anti-mouse IgG-HRP (BioLegend) at a dilution of 1:1000.

Tissue harvest and blood analyses. Harvest was performed by the Comparative Pathology Core of the Veterinary Hospital of the University of Pennsylvania. Blood samples were collected by cardiocentesis into lithium heparin tubes for automated complete blood count analysis (IDEXX ProCyte Hematology Analyzer) and clinical chemistry (Vitros 4600 Chemistry System analyzer, Ortho Clinical Diagnostics). Blood smears were prepared for manual pathology review of leukocyte differential counts and morphology assessment as needed. Degree of hemolysis was visually assessed and graded by a laboratory technician.

Necropsy samples included spleen, liver, kidney, skin/oral mucosa, urinary bladder, heart, lung, stomach, colon, brain, and testis, immersion-fixed in 4% paraformaldehyde solution (ThermoFisher) or 10% neutral buffered formalin (ThermoFisher) prior to processing.

Immunohistochemistry (IHC) was performed for human CD3 (Bio-Rad, clone MCA1477T, 1:500 dilution, and mouse CD79b (CST, clone 96024, 1:300 dilution) using a fully automated BOND RXm (Leica Biosystems).

For flow cytometry, cells from whole blood were stained with anti-CD3 BV650 (OKT3, BioLegend) with CountBright Absolute Counting Beads (ThermoFisher) and fixed with FacsLyse solution (BD).

Direct immunofluorescence analysis. Mucosa was harvested on day 17, embedded in OCT (Tissue-Tek), and frozen at -80ºC. Cryosections were washed in PBS then blocked in PBS with calcium and magnesium (PBS/Ca, Gibco) containing 2% BSA for 60 minutes, incubated with FITC-conjugated goat anti-mouse IgG (Rockland Inc.) at a 1:200 dilution in blocking solution for 1 hour at room temperature, then washed with PBS/Ca. Binding of anti-DSG3 IgG was visualized with an Olympus BX61 microscope equipped with a Hamamatsu Orca ER camera using Slidebook 4.2 software (Olympus).

Quantitative PCR (qPCR). qPCR was performed by the Translational and Correlative Sciences Laboratory (TCSL) (*41*). Briefly, genomic DNA was isolated from spleen, and qPCR analysis was performed using a validated ABI TaqMan assay to detect the integrated BBZ transgene sequence (*42*). The number of copies of plasmid present in the standard curve was verified using digital qPCR with the same primer/probe set and performed on a QuantStudio 3D digital PCR instrument (Life Technologies). Datapoints were evaluated in triplicate with a positive Ct value in three of three replicates with percent coefficient of variation of less than 0.95% for all quantifiable values. To control for DNA quality, a parallel amplification reaction was performed using 20 ng of genomic DNA and a primer/probe combination specific for a non-transcribed genomic sequence upstream of the CDKN1a (p21) gene as described(*42*). These

amplification reactions generated a correction factor to adjust for calculated versus actual DNA input. The average marking per human cell was defined as: (copies of plasmid/input DNA in ng) x p21 correction factor x 0.00063 ng DNA/mammalian cell x amplification-specific correction factor.

Active immune PV model. All in vivo studies were performed under approved IACUC protocols. DSG3$^{-/-}$DSG1$^{tg/tg}$ mice on a C57Bl/6J background (hereafter abbreviated as DSG3 KO), were maintained by mating DSG3 KO mice aged 3 to 4 months.

Immunization of DSG3-deficient mice with rhDSG3. DSG3 KO mice were immunized subcutaneously with 10 μg rhDSG3 (Euroimmun) in complete Freund's adjuvant (Sigma-Aldrich) on day 0, in incomplete Freund's adjuvant (Sigma-Aldrich) on days 7 and 14, and in PBS on days 21, 28, 35, and 42.

ELISA. Standard DSG3 ELISA (Euroimmun) used a 2:98 dilution of mouse serum and HRP-conjugated rabbit anti-mouse IgG diluted at 1:3000 (BioLegend). Sera from a previously immunized or non-immunized DSG3 KO mouse was used as a positive or negative control standard.

To estimate the level of serum anti-DSG3 antibodies relative to human patients, anti-human IgG (Euroimmun) or HRP-conjugated donkey anti-mouse IgG (Abcam) secondary antibody reagents were normalized against known quantities of mouse IgG1 (Sigma), human IgG1 (Athens Research & Technology), human IgG4 (Sigma) and human IgG (Sigma), to obtain equivalent optical density (OD) readings when equal quantities of mouse and human IgG are bound. Subsequently, mouse sera (1:20 or 1:100) and donkey anti-mouse IgG-HRP (1:4000) was

run in parallel with standard control reagents using the human DSG3 ELISA, and index values (RU/ml) were calculated according to manufacturer's recommendations.

Adoptive transfer of mouse splenocytes from DSG3 KO mice immunized with rhDSG3. 6-7 weeks after rhDSG3 immunization, spleens were harvested, diced into 0.5 mm cubes, and pressed through a 75 nm strainer in 10 mL ice cold PBS. Cells were harvested by centrifugation at 500xg for 5 minutes, washed, and resuspended in 2 mL of 37°C lysis buffer (BD PharmLyse). Splenocytes were subsequently washed and resuspended in ice-cold PBS at a concentration of $3x10^7$ cells per mL. 3-5 x 10^6 splenocytes were adoptively transferred by intravenous injection into $RAG2^{-/-}$ mice.

Flow cytometric analysis of mouse splenocytes. Antibodies for analysis included anti-B220 APC (clone RA3-6B2), anti-CD4 PE (clone GK1.5), and anti-CD8α Alexa Fluor 700 (clone 53-6.7), all from BioLegend.

Mouse ELISPOT. Plates were coated as above and blocked with PBS/Ca containing 1% BSA. Control hybridomas or mouse splenocytes were added to wells in PFHM-II medium (Gibco) and cultured for 8 hours at 37°C with 5% CO_2. Spots were detected with a biotinylated anti-mouse IgG and avidin-HRP (MabTech), followed by TMB solution (MabTech). Quantitation of the percent of DSG3-reactive splenocytes was performed by dividing the number of spots detected in wells coated with rhDSG3 by the normalized number of spots in wells coated with anti-mouse IgG, including only values that fell within the quantifiable range of the assay.

Epitope mapping. 5 μL mouse sera were added to 293T-cell culture supernatant containing human DSG3-DSG2 domain-swapped molecules, pre-cleared against protein A beads (Invitrogen). Protein A beads were used to precipitate the IgG bound to the DSG3-DSG2 molecules, followed by SDS-PAGE and immunoblotting with anti-E-tag antibody (Abcam).

Evaluation of DSG3-CAART efficacy. 20 days after adoptive transfer of splenocytes, 10 and 5 mice were treated with $3x10^6$ DSG3-CAART or NTD T-cells by intravenous injection, respectively. NTD- and 5 DSG3-CAART-treated mice were euthanized at day 39 (or earlier based on humane endpoints as above); 5 DSG3-CAART-treated mice were euthanized at day 69.

Tissue harvest and ex vivo flow cytometry analysis. Skin and oral mucosa were harvested and fixed in either 4% formalin for hematoxylin and eosin (H&E) staining by the Penn Skin Biology and Diseases Resource-based Center, or embedded in OCT (Tissue-Tek) and frozen at -80°C for direct immunofluorescence analysis. Flow-cytometric analysis of peripheral blood T-cells was performed with CountBright absolute counting beads (Thermo Fisher).

In vitro assays for redirected lysis of Fc-receptor-expressing cells.

Expression of CD16a, CD32a, CD64 Fc gamma receptors (FcγRs) in K562 cells. CD32a (FcγRIIa)- and CD64 (FcγRI)-expressing K562 cells (provided by Carl June, University of Pennsylvania, Philadelphia, USA) were transduced with click-beetle green luciferase. K562 cells (ATCC) were transduced with lentivirus encoding CD16a (FcγRIIIa) and click beetle green luciferase. After transduction, cell lines were sorted to select for high expression. Using PE QuantiBrite beads (BD) for quantification, K562 cells engineered to express FcγRs or primary human monocytes or natural killer (NK) cells from healthy donors (Penn Human Immunology Core) were stained with anti-human CD16 (clone 3G8), CD32 (clone FUN-2), or CD64 (clone 10.1)-PE (all from BioLegend, fluorescence to protein (F/P) ratio ~1) under saturating conditions for 30 minutes at 4°C, washed, then analyzed by flow cytometry (LSRII, BD). Average surface area of K562 cells, primary monocytes and NK cells was obtained by a Multisizer 4e (Beckman Coulter) to calculate the density.

PV IgG purification. PV plasma was obtained from otherwise discarded plasmapheresis samples from PV patients according to Institutional Review Board approved protocols. PV IgG was purified using a Melon Gel IgG purification kit (ThermoFisher Scientific) or by protein A chromatography (Invitrogen) according to manufacturer's recommendations. Antibodies used for pre-incubation with target cells included mouse anti-human CD3 (clone OKT3, Thermo Scientific), normal human IgG (Sigma), and IVIG as normal human IgG (Privigen).

Flow-based indirect cytotoxicity assay on primary human monocytes and NK cells.

Monocytes/NK cells were stained with anti-human CD64 BV421 (clone 10.1) or anti-human CD16 PE (clone 3G8, both from BioLegend) respectively. Effector T-cells (NTD or DSG3-CAART) were stained with anti-human CD4 BV510 (clone OKT4, BioLegend) and anti-human CD8 APC/CY5.5 (clone RFT8, Southern Biotech). After washing, monocytes/NK cells were resuspended in media with purified PV IgG at 50-150 RU/mL plus effector T-cells at effector to target (E:T) ratio of 10:1. The NH IgG amount was matched to the equivalent amount of PV IgG, and OKT3 concentration was 1% of the total IgG amount. In the 20 RU/mL condition, monocytes and NK cells were pre-coated with PV IgG that had a titer of 20 RU/mL or equivalent amount of NH IgG or OKT3 for 30 minutes on ice. After washing, PV and NH IgG was added back to the target cells and transferred to effector T-cells at E:T ratio of 10:1, co-incubated for 4 hours at 37°C, and analyzed by flow cytometry (LSR II, BD), using propidium iodide to evaluate cell viability.

Luciferase-based cytotoxicity assays using K562 cells. FcγR-expressing K562 cells were co-cultured with DSG3-CAART or NTD T-cells at E:T ratios of 3:1 or 10:1 in the presence of PV IgG, NH IgG, or OKT3. In the 20 RU/ml condition, target cells were incubated with either 20 RU/mL PV IgG, or equivalent amount of NH IgG or OKT3 for 30 minutes on ice. After

washing, FcγR-expressing K562 cells were added to DSG3-CAART or NTD T-cells at E:T ratios of 3:1 or 10:1 in the presence of a final concentration of 0.33 μg/mL PV IgG, normal human IgG, or OKT3. At 4 hours, luciferase substrate (D-luciferin potassium salt, GoldBio) was directly added to each well and emitted light (relative luminescence units) was measured on a luminescence plate reader (Synergy HTX microplate reader, BioTek). Target cells incubated in medium alone or with 5% SDS were used to determine maximum or minimum luminescence emission, respectively. Percent specific lysis was calculated as follows: 100 x (maximum RLU – experimental RLU)/ (maximum RLU – minimum RLU).

IFNγ ELISA. Supernatants were collected after 20-24 hours of co-culture and stored at -80°C prior to analysis with the Human IFN gamma DuoSet ELISA (R&D Systems) at a sample dilution of 1:50.

Assessment of DSG3-CAART IFNγ production and cell clustering in response to soluble anti-DSG3 antibody. NTD, CART19 or DSG3-CAART cells (400 μL at $1x10^6$/mL) were cultured in duplicate with medium or PV serum IgG (50-200 RU/mL). After 20-24 hours, images were acquired with an EVOS FL followed by posteriori cell clustering analysis using ImageJ. Cytokine production in culture supernatants was assessed with the Human IFN gamma DuoSet ELISA (R&D Systems) using a sample dilution of 1:100.

Quantitative PCR. mRNA was isolated from primary cells, and cDNA was produced using reverse transcriptase. qPCR was performed with a QuantStudio 3D PCR system (Applied Biosystems) using TaqMan® assays (Thermo-Fisher) with normalization to internal controls (GAPDH). Results were calculated according to the following formula: 1/(2^[-Delta Ct]). Probes

included GAPDH (Hs02758991_g1), DSC1 (Hs00245189_m1), DSC2 (Hs00951428_m1), DSC3 (Hs00170032_m1), CLEC4M (Hs03805885_g1). Data was analyzed using AnalysisSuite™ Cloud Software (Applied Biosystems).

Luminex multiplex cytokine assay. DSG3-CAART or donor-matched NTD T-cells were co-cultured (E:T ratio 0.3:1) with target cells for 24 hours, followed by harvest of co-culture supernatants to quantify expression of EGF, FGF-2, Eotaxin, sIL-2Ra, G-CSF, GM-CSF, IFN-a2, IFN-G, IL-10, IL-12p40, IL-12p70, IL-13, IL-15, IL-17A, IL-1Ra, HGF, IL-1b, CXCL9/MIG, IL-2, IL-4, IL-5, IL-6, IL-7, CXCL8/IL-8, CXCL10/IP-10, CCL2/MCP-1 CCL3/MIP-1a, CCL4/MIP-1b, CCL5/RANTES, TNF-alpha, and VEGF, using a FlexMap 3D instrument (Luminex) with a Luminex bead array platform (Millipore Sigma) according to the manufacturer's instructions. Positive controls consisted of DSG3-CAART cells co-cultured with Nalm-6 PVB28 cells. Negative controls consisted of donor-matched NTD cells co-cultured with the same targets, targets alone, and media alone. Samples were analyzed in duplicate and compared against multiple internal standards, with a nine-point standard curve using xPONENT software (Luminex).

xCELLigence real-time cell analysis.

Cells/media: Complete Epithelial Growth Medium: colon (H-6047), kidney (H-6034), stomach (H-6039) (Cell Biologics), and bladder (PCS-420-010, ATCC). Renal cortical (C-12660), cardiomyocytes (C-12811), and small airway (C-12642) epithelia with respective growth media: PromoCell. Pulmonary microvascular (H-6011) and hepatic sinusoidal (H-6017) endothelial cells, Complete Endothelial Cell Growth Medium: Cell Biologics.

Impedance assays: Primary human cells were cultured on gelatin-coated flasks and used at passage 3 for assays. Cells were seeded in duplicate into 96-well polyethylene terephthalate plates (E-Plate VIEW 96 PET, Acea Biosciences) at 5,000 cells/well and allowed to adhere for 24 hours. Nalm-6 PVB28 cells were tethered to wells via anti-CD9 capture antibodies according to the manufacturer's instructions. Adhesion or tethering of cells to the gold microelectrodes in the E-Plates impedes the flow of electric current between electrodes. Effector cells (DSG3-CAART or NTD cells) were added to wells at E:T cell ratios of 50:1, 25:1, 10:1 and 1:1. Target cells lysed by 1% Triton X-100 were used as the positive control, while donor-matched NTD cells at the same E:T ratios were assayed as negative controls. Impedance data was continuously acquired over 7 days and analyzed using RTCA 2.1.0 software. Curves indicate the % Cytolysis using NTD controls as a reference, after subtracting the signal from wells containing effector cells alone and from wells containing target cells treated with a rapid killing agent (i.e., Triton X-100) to compensate for residual background signal. The equation for calculating the % Cytolysis for a sample *s* at a timepoint *t* is: $\%\ \text{Cytolysis}_{st} = [1-(NCI_{st})/(\text{Avg}NCI_{Rt})]x100$, where NCI_{st} is the Normalized Cell Index for the sample and NCI_{Rt} is the average of the Normalized Cell Index for the matching reference wells.

Membrane proteome array screen.

Production of DSG3EC1-4-Fc-his: Soluble DSG3EC1-4-Fc-his was synthesized (IDT) and cloned into the pHEK293 Ultra Expression Vector I (TakaraBio) for transient transfection into HEK293T cells (ATCC CRL-11268) using Lipofectamine 2000 (ThermoFisher) according to manufacturer's protocols. Protein was purified from culture supernatants by metal affinity chromatography (HisPur Cobalt Resin, ThermoFisher) according to manufacturer's protocols,

dialyzed into PBS with calcium and magnesium (Gibco), quantitated by Coomassie standard against a BSA control, and stored in aliquots at -80°C. Protein conformation and identity was confirmed by ELISA using (D31)2/29) (Px43) and (D31)12b/6 (Px44) scFv mAbs(*41*), as well as immunoblot for the DSG3 and Fc-domains.

Membrane Proteome Array (MPA, Integral Molecular): To identify DSG3EC1-4-Fc-his binding targets, 5300 different membrane proteins were each expressed in individual wells of HEK293T cells arrayed in 384 well plates. The cells were matrixed by pooling individual columns and rows of each 384 well plate, followed by permeabilization using a proprietary method that does not require fixation. To determine optimal screening conditions, different concentrations of soluble DSG3EC1-4-Fc-his were tested on HEK293T cells expressing a membrane-bound protein A construct, DSC2, DSG2, DSG-CAAR, Px44 membrane-bound single chain variable fragment antibody, or vector alone (pUC), using a single dilution of secondary and tertiary antibodies. Optimal screening concentrations were determined by the background signal (mean fluorescence intensity (MFI) and false positive rate in the vector control.

DSG3EC1-4-Fc-his binding to overlapping column and row pools was evaluated. Each individual membrane protein target was assigned values corresponding to the binding values of their unique row and column pools. The resulting paired binding values were subsequently normalized and transformed to give a single numerical value for binding of the DSG3EC1-4-Fc-his protein against each target protein. Non-specific fluorescence was defined as any value below 3 standard deviations of the mean background value.

To validate protein targets identified in the MPA, HEK293T cells were transfected with plasmids expressing the respective targets or vector alone (negative control). Serial dilutions of

each mAb were then tested for immunoreactivity against cells over-expressing the identified target protein. The Fc-isotype control was an unrelated Fc-fusion protein (PD-L1-Fc, R&D Systems). MFI of the target must exceed that of the Fc-isotype control by 2-fold to be considered positive on the validation screen.

Evaluation for IFNγ production by DSG3-CAART following exposure to CLEC4M-expressing cells.

CLEC4M construction. The CLEC4M v8 sequence was derived from pCDNA3-CLEC4M v8 (Integral Molecular) as template. The CLEC4M v8 was amplified using the following primers: 5'-TAAGCAGGATTATGAGTGACTCCAAGGAACCA-3' and 5'-TGCTTAGTCGACCTATTCGTCTCTGAAGCAGGCTGC-3' and then cloned into the pCLPS vector, a third generation self-inactivating CMV promoter based lentiviral expression vector based on pRRL-SIN-CMV-eGFP-WPRE where eGFP was replaced by CLEC4M v1 or v8.

Transduction and sorting of K562 cells. pCLPS was modified to express CLEC4M v1 or v8 followed by lentiviral production. K562 cells were cultured in a 6-well plate at $1x10^6$ cells in 5 ml of RPMI culture media and transduced with CLEC4M v1 or v8 lentivirus. After resting cells for 24-48 hours, cells were expanded and sorted to select for high expression of CLEC4M v1 or v8 (Tyto, Miltenyi).

Cytokine ELISA. IFNγ production was quantified by ELISA (Human IFNγ DuoSet ELISA, R&D Systems), according to the manufacturer's recommendations, in duplicate culture supernatants after co-culture of $1x10^5$ DSG3-CAART or CART19 effector cells with 10^4 Nalm6-CD19, Nalm6-PVB28, K562-CLEC4M v1 or K562-CLEC4M v8 target cells at an E:T of 1:2, 1:1, 1:0.5 and 1:0.25 for 16 hours.

Patient T-cell manufacturing and phenotyping

Patient characteristics and venipuncture: Venipuncture and clinical chart review was performed under IRB-approved protocols. PV patients were subjectively categorized as receiving "low", "moderate" or "heavy" immunosuppression as follows (daily doses indicated):

- Low: Prednisone 7.5 mg (2 patients)
- Moderate: azathioprine 50 mg + prednisone 10 mg
- Heavy: mycophenolate mofetil 3000 mg + prednisone 40 mg; prednisone 40 mg alone

ALC was obtained from hematologic profiles as part of routine clinical monitoring in 31 pemphigus patients on standard immunosuppressive therapies who had not received rituximab within the 12 months prior to blood draw.

T-cell isolation: Peripheral blood mononuclear cells (PBMCs) were isolated from heparinized blood by Ficoll gradient centrifugation, frozen in 90% FBS, 10% DMSO, and stored at -170°C. PBMCs were thawed and T-cells were isolated by negative selection using the EasySep Human T-cell Isolation Kit (StemCell Technologies). Generation of patient DSG3-CAART cells followed methods described above.

Luciferase-based cytotoxicity assay: Nalm6 target cells were co-cultured with DSG3-CAART or NTD T cells at various E:T ratios for 18-22 hours and percent specific lysis was calculated as described above.

PBMC phenotyping: Mouse anti-human antibodies included: anti-CCR7 FITC (clone 150503), anti-PD1 PerCP/Cy5.5 (clone EH12.1), anti-CD69 APC (clone FN50), anti-CD19 BV421 (clone HIB19), anti-CD27 PE-Cy7 (clone M-T271) from BD Biosciences; anti-TIM3 Alexa Fluor700 (clone 344823) from R&D Systems; anti-CD8 APC-Cy7 (clone SK1), anti-CD4

BV510 (clone SK3), anti-CD3 BV605 (clone OKT3), anti-CD127 BV711 (clone A019D5), anti-CD14 BV785 (clone M5E2), anti-CD45RO PE (clone UCHL1), anti-CD95 PE-Cy5 (clone DX2) from BioLegend. Patient PBMCs were thawed, washed in PBS, and stained for 30 minutes at room temperature. Populations of interest were gated based on forward versus side scatter characteristics followed by singlet gating, and live cells were gated using Live Dead Fixable Aqua (Invitrogen, LifeTechnologies).

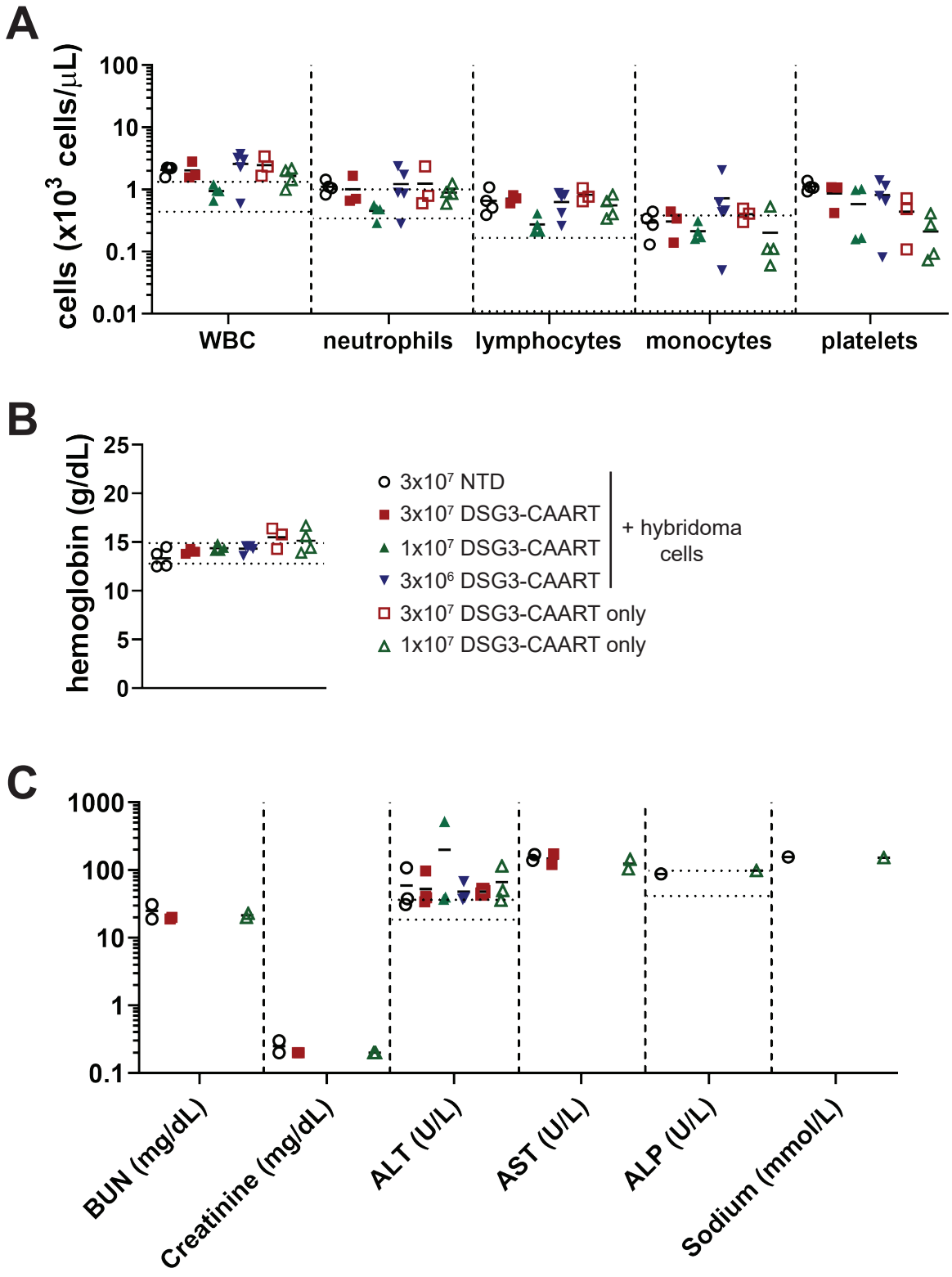

Supplementary Figure 1. Complete blood count and serum chemistry analysis of NTD and DSG3-CAART treated mice in a PV mixed hybridoma model. (A) White blood cell count (WBC), (B) hemoglobin level, and (C) serum chemistries are shown. $3x10^7$ (red squares), $1x10^7$ (green triangles), and $3x10^6$ (blue triangles) DSG3-CAART cell doses show comparable values to NTD control-treated mice (black circles). Mean value of each group is shown with a black line. Reference limits for NSG mice are bracketed with black dashed lines.

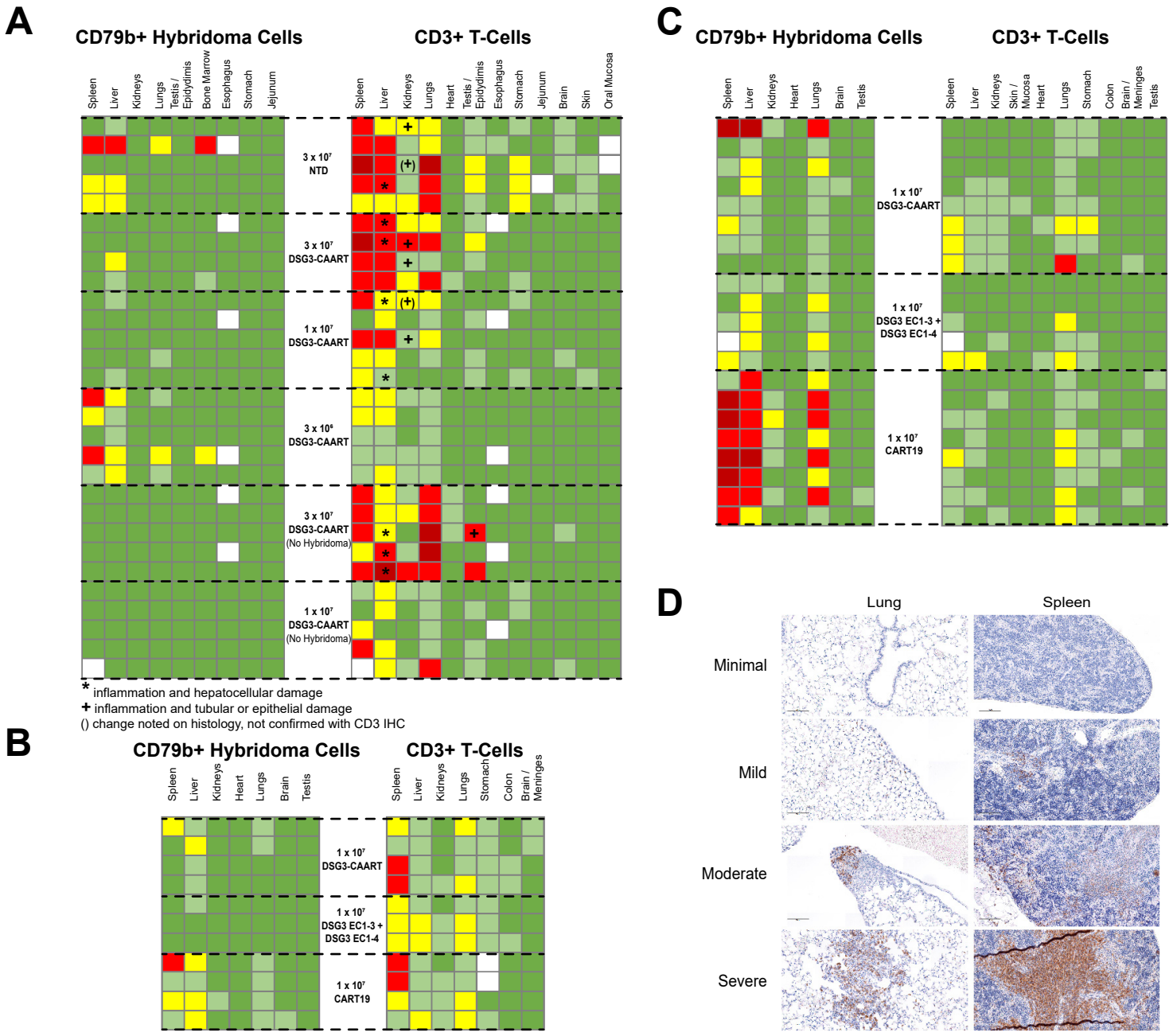

Supplementary Figure 2. Treatment with DSG3-CAART, CART19, or NTD T-cells in a PV mixed hybridoma model results in comparable levels of inflammatory cell infiltrates in internal organs at different dose levels and harvest time points. DSG3-CAART toxicology was evaluated in a PV mixed hybridoma model to evaluate whether off-target cytotoxicity may occur with increasing DSG3-CAART doses or at different time points corresponding to peak T-cell expansion or subacute engraftment. CD3+ T-cell and CD79b+ hybridoma cell infiltrates were systematically evaluated by immunohistochemistry (IHC) analysis of harvested tissues from (A) the dose-activity experiment shown in Figure 2, and a separate study investigating (B) acute (day 7 after T-cell injection) and (C) subacute (day 15 after T-cell injection) toxicology as described in Methods. Colors indicate degree of cell infiltration: green (none), light green (minimal), yellow (mild), red (moderate), dark red (severe). Occasional parenchymal changes (single hepatocyte necrosis, renal tubular dilation, degeneration, necrosis, and intraepithelial epididymal T-cells) were observed in some DSG3-CAART or NTD treated mice as indicated. CD79b+ hybridoma cell staining indicates control of hybridoma outgrowth in most DSG3-CAART- compared to CART19-treated mice. (D) Representative images from lung and spleen demonstrating the degree of T-cell infiltration classified as minimal, mild, moderate, or severe.

A

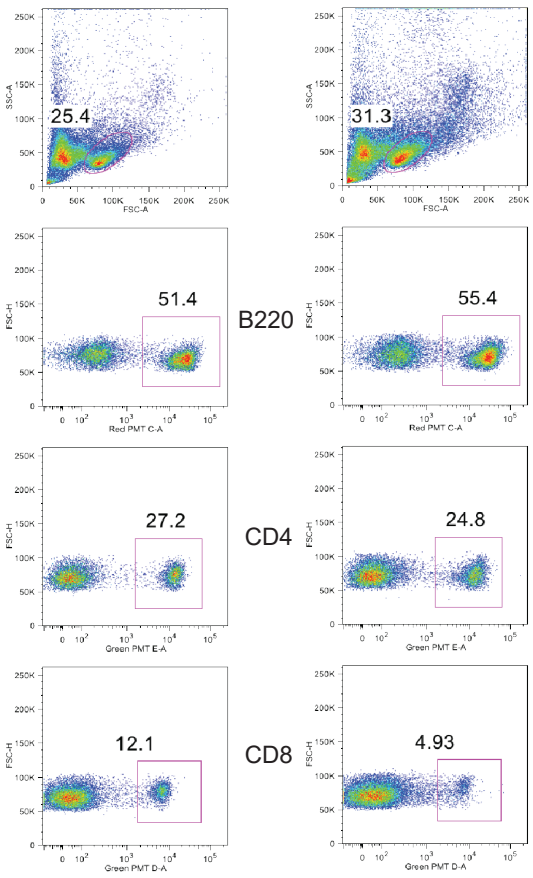

B

# spots / X cells	# spots rhDSG3	# spots anti-mouse IgG (normalized)	% DSG3-reactive splenocytes
1000	122	340	35.9%
2000	185	542	34.1%
4000	405	984	41.2%

C

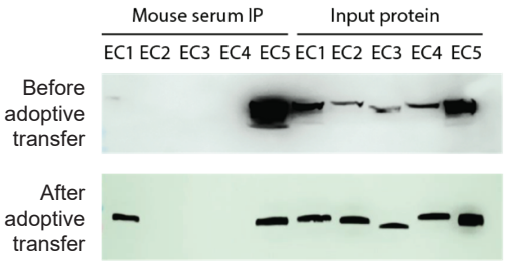

D

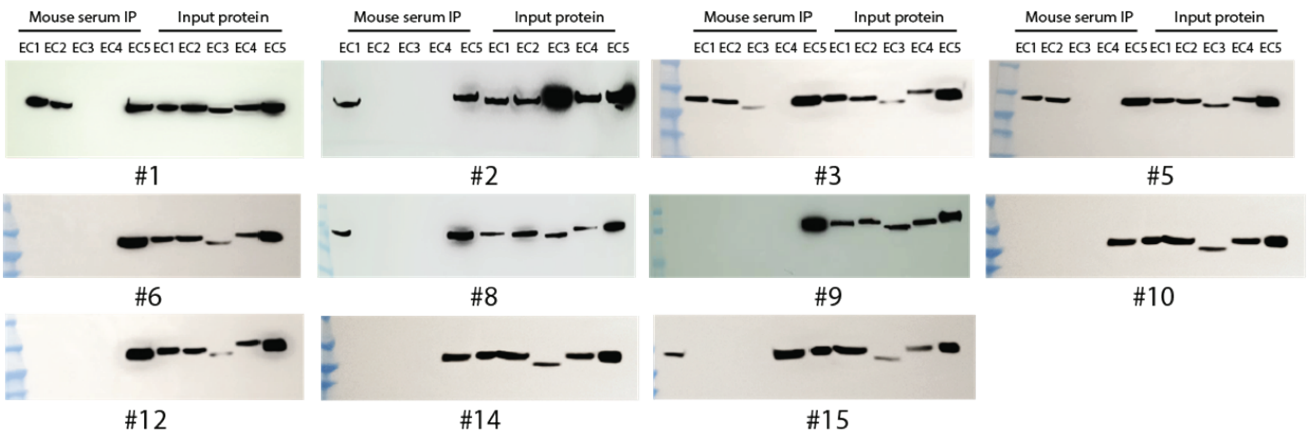

Supplementary Figure 3. rhDSG3 immunization of DSG3 KO mice for generation of a human DSG3-reactive active immune model of PV. (A) Flow cytometric analysis of splenocytes after rhDSG3 immunization. (B) Calculation of percent DSG3-reactive splenocytes determined by ELISpot. (C) Epitope mapping of serum antibodies from one DSG3 KO mice immunized with rhDSG3 at the time of splenocyte harvest (week 7) and 3 weeks after adoptive transfer to a RAG2-deficient mouse. Immunoprecipitation-immunoblot to evaluate serum reactivity is shown in the left 5 lanes, and input protein for each of the EC domain-swapped constructs is shown in the right 5 lanes of each panel for reference. (D) Epitope mapping of NTD (#1-5) and DSG3-CAART treated (#6-15) mice at the time of harvest. Epitope mapping was not performed on mice #4, #7, #13 due to unexpected death or weight loss requiring euthanasia and mouse #11 due to insufficient serum.

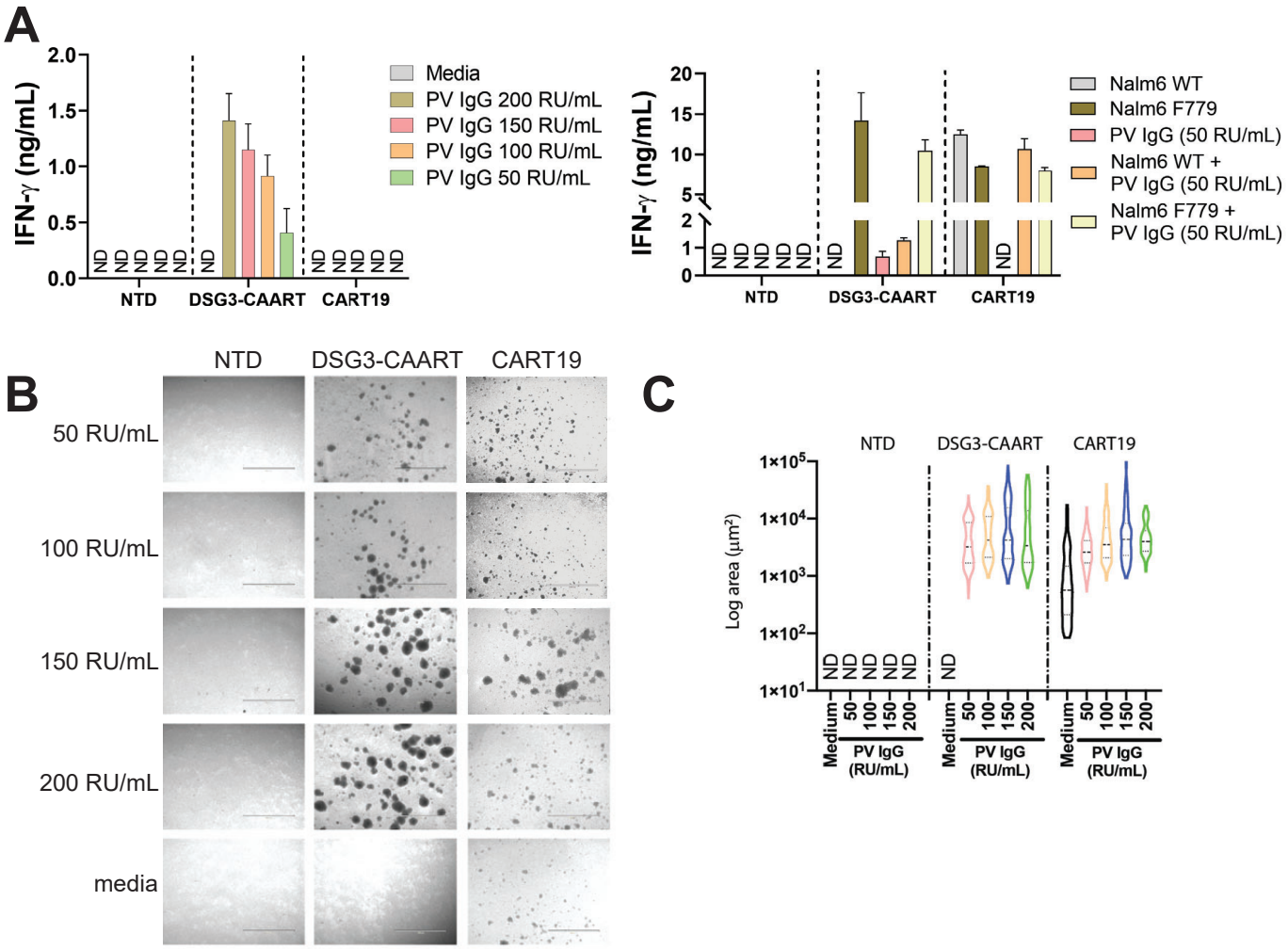

D

	Medium	50 RU/mL	100 RU/mL	150 RU/mL	200 RU/mL
NTD	ND	ND	ND	ND	ND
DSG3-CAART	ND	2789.6 (1571.8-7752.9)	4206.0 (2124.5-10785.0)	4221.2 (2018.1-15302.6)	3357.1 (1720.1-13691.2)
CART19	569.4 (216.4-1458.0)	2554.5 (1714.7-4127.5)	3250.3 (2107.1-5182.8)	4352.4 (2295.7-7936.5)	3986.9 (2764.2-6186.6)

Supplementary Figure 4. PV serum IgG activates DSG3-CAART cytokine production and homotypic clustering. (A) PV serum IgG induces titer-dependent IFNγ production from DSG3-CAART but not NTD or CART19 T-cells. T-cells were incubated with PV IgG (50, 100, 150 or 200 RU/mL, left panel) or with an equal number of target cells (Nalm6 WT or Nalm6 F779) + 50 RU/mL PV IgG (right panel) and IFNγ was quantitated by ELISA in cell culture supernatants 24 hours later. Bars represent average of duplicate samples; error bars indicate standard deviation. ND, Not Detectable. (B) Microscopy images of NTD, CART19 and DSG3-CAART cells stimulated with medium alone or PV IgG (50, 100, 150 or 200 RU/mL) demonstrate homotypic clustering in response to PV IgG. Scale bar = 1000 μm. (C) Quantification of cell cluster size using ImageJ. Violin plots represent the frequency distribution of the cell clusters for each sample and treatment, with median and interquartile range indicated with dashed lines. (D) Median (interquartile range) for cell cluster size (μm^2) shown in (B).

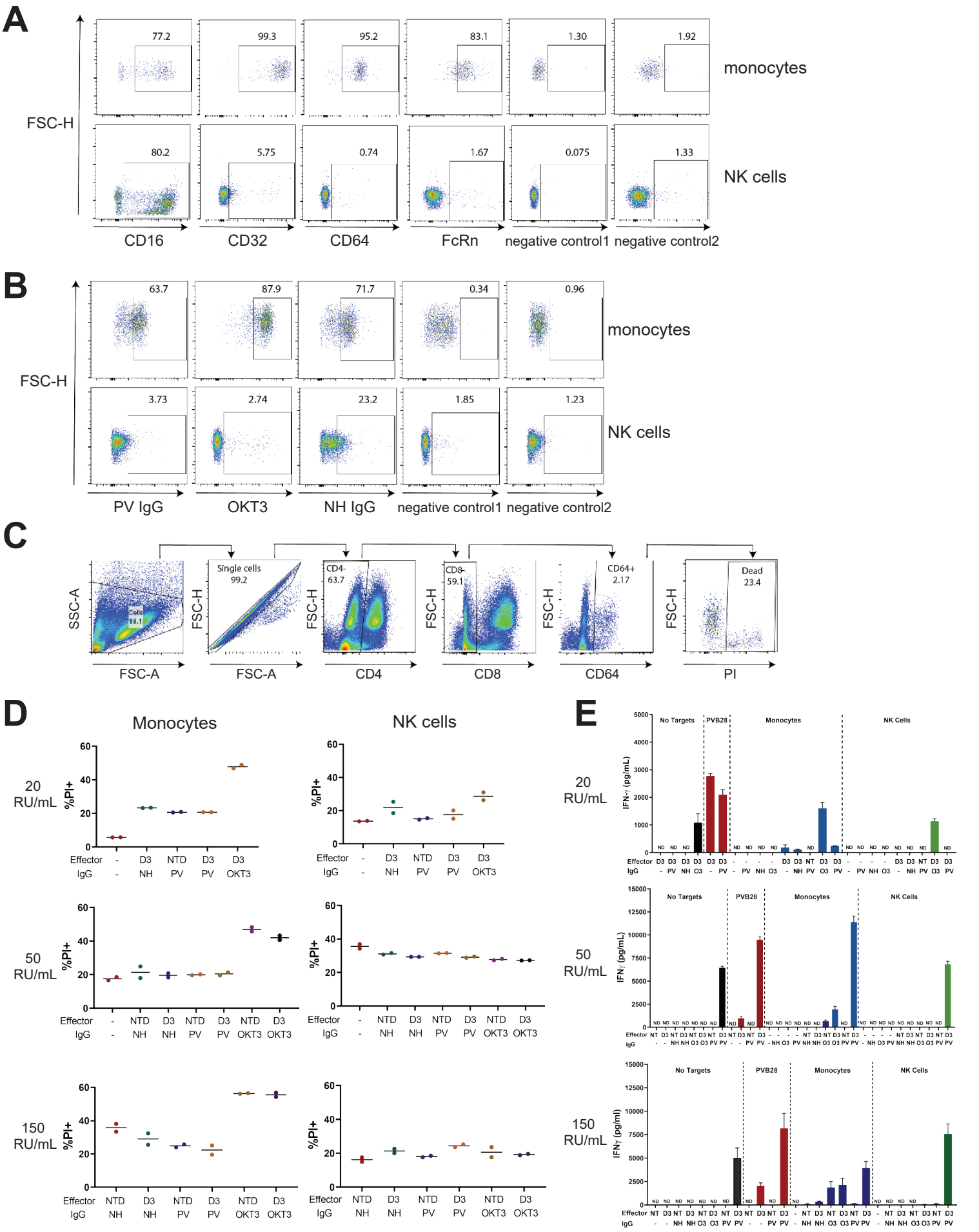

Supplementary Figure 5. DSG3-CAART cells do not demonstrate redirected lysis of primary human monocytes and NK cells in the presence of PV IgG. (A) Monocytes express CD16, CD32, CD64 and FcRn, whereas NK cells only express CD16. Negative control 1, isotype control for CD16, CD32, CD64. Negative control 2, secondary antibody alone (control for FcRn). Data is representative of 3 independent experiments with different donors. (B) Monocytes demonstrate sIg staining whereas NK cells have minimal to no sIg binding after pre-incubation. Negative control 1, anti-mouse IgG secondary antibody alone (control for OKT3). Negative control 2, anti-human IgG secondary antibody alone (control for PV and NH IgG). Data is representative of 3 independent experiments with different donors. (C) Overview of gating strategy for monocytes. CD4-CD8-CD64+ populations were gated and evaluated for cell death via PI staining.The same gating strategy was used for NK cells except the CD16+ (rather than CD64+) population was selected. (D) The percentage of monocytes or NK cells that are PI-positive (% PI+), which measures target cell death. Horizontal lines represent the average of duplicate samples. Double negative indicates monocytes or NK cells alone. (E) IFNγ levels after 20 hours of co-incubation of monocytes or NK cells with target cells and PV IgG at an E:T ratio of 10:1. The average of duplicate values is shown with error bars to indicate the range of values. O3, OKT3; NT, NTD; D3, DSG3- CAART.

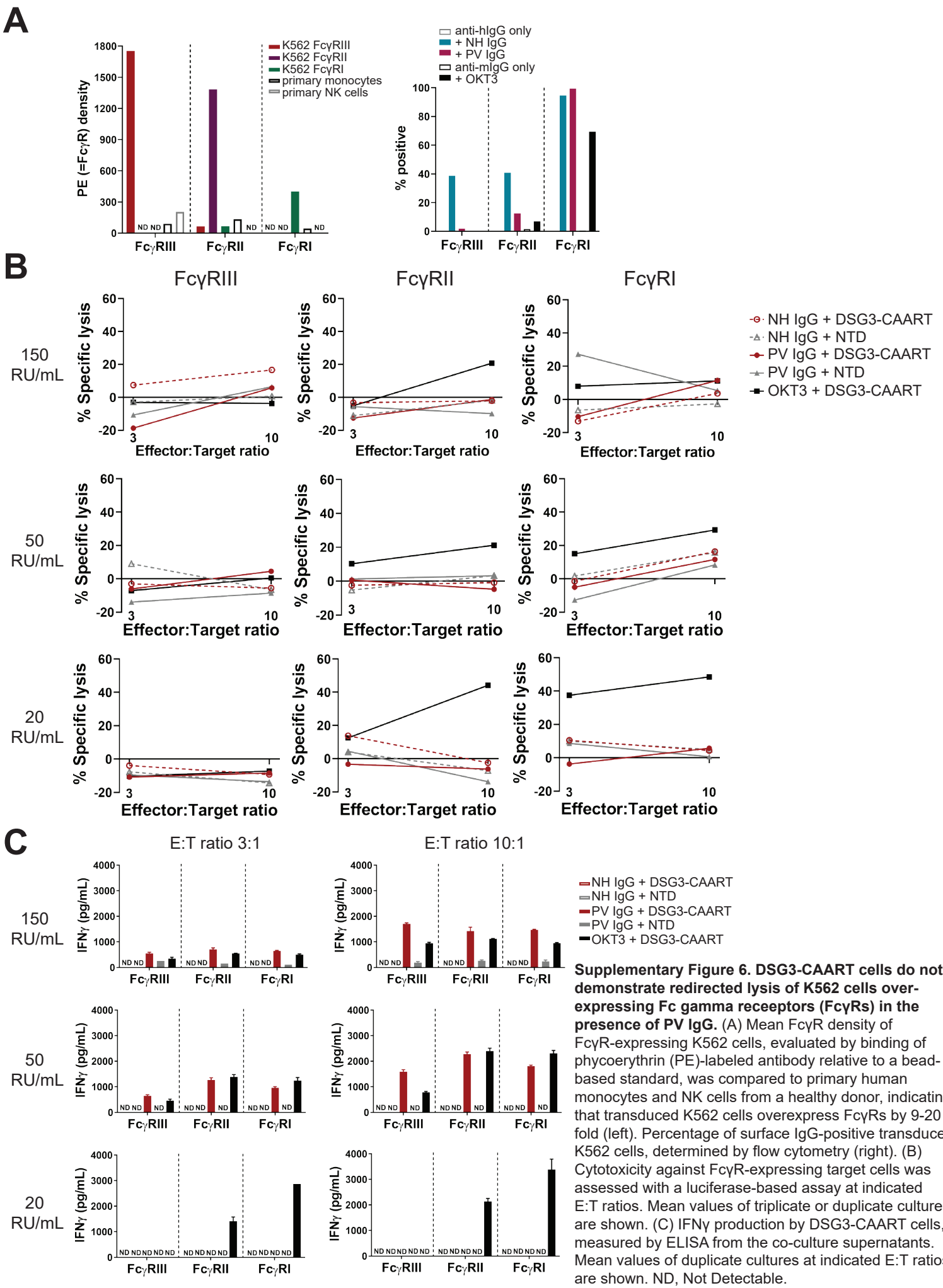

Supplementary Figure 6. DSG3-CAART cells do not demonstrate redirected lysis of K562 cells over-expressing Fc gamma receeptors (FcγRs) in the presence of PV IgG. (A) Mean FcγR density of FcγR-expressing K562 cells, evaluated by binding of phycoerythrin (PE)-labeled antibody relative to a bead-based standard, was compared to primary human monocytes and NK cells from a healthy donor, indicating that transduced K562 cells overexpress FcγRs by 9-20 fold (left). Percentage of surface IgG-positive transduced K562 cells, determined by flow cytometry (right). (B) Cytotoxicity against FcγR-expressing target cells was assessed with a luciferase-based assay at indicated E:T ratios. Mean values of triplicate or duplicate cultures are shown. (C) IFNγ production by DSG3-CAART cells, measured by ELISA from the co-culture supernatants. Mean values of duplicate cultures at indicated E:T ratios are shown. ND, Not Detectable.

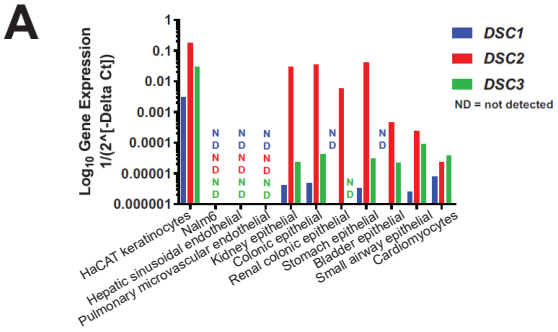

Supplementary Figure 7. DSG3-CAART does not demonstrate specific off-target cytotoxic interactions with primary human desmosome-expressing cells. (A) DSC1, DSC2, and DSC3 mRNA levels in primary human cells derived from desmosome-expressing tissues were assessed, using Nalm6 B-cells and hepatic sinusoidal and pulmonary microvascular endothelial cells as negative controls for desmocollin expression. GAPDH served as a loading control. (B) Multiplex analysis of 31 soluble cytokines, chemokines, and growth factors in the supernatants of DSG3-CAART cells co-cultured with Nalm6 PVB28 cells (positive control) or primary human desmosome-expressing cells. Levels of cytokines produced in excess of those from donor-matched NTD T-cell controls are shown. IFNγ and TNFα production typically reflect cytotoxic stimulation and are elevated for Nalm6 PVB28 cells, (red arrows) but no other cells, relative to NTD controls. (C) xCELLigence real-time assay of DSG3-CAART co-cultured with primary human desmosome-expressing cells at E:T ratios of 50:1 (red), 25:1 (blue), 10:1 (orange) and 1:1 (green. Percent cytolysis reflects changes in cellular impedance of target cell monolayers.

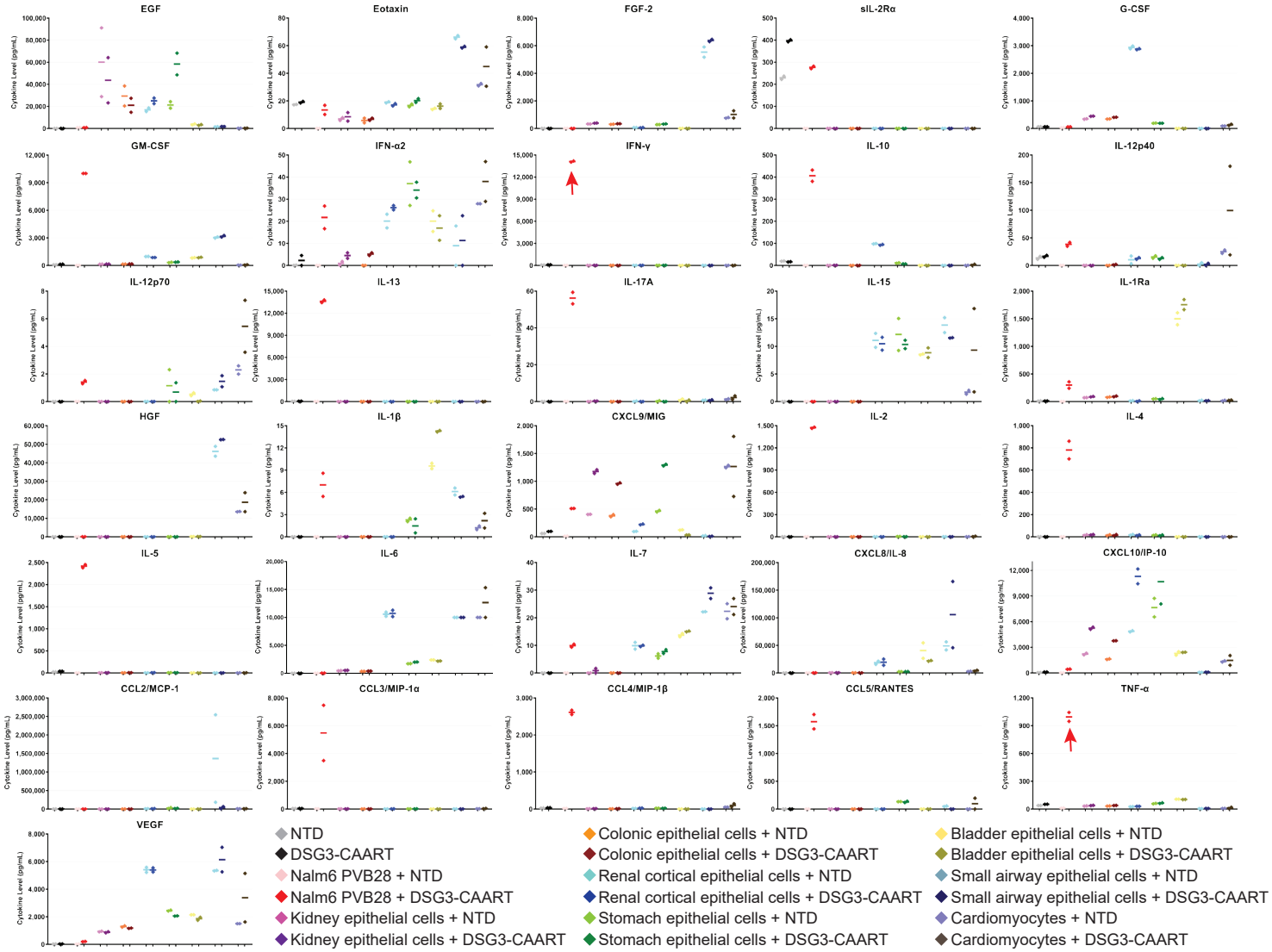

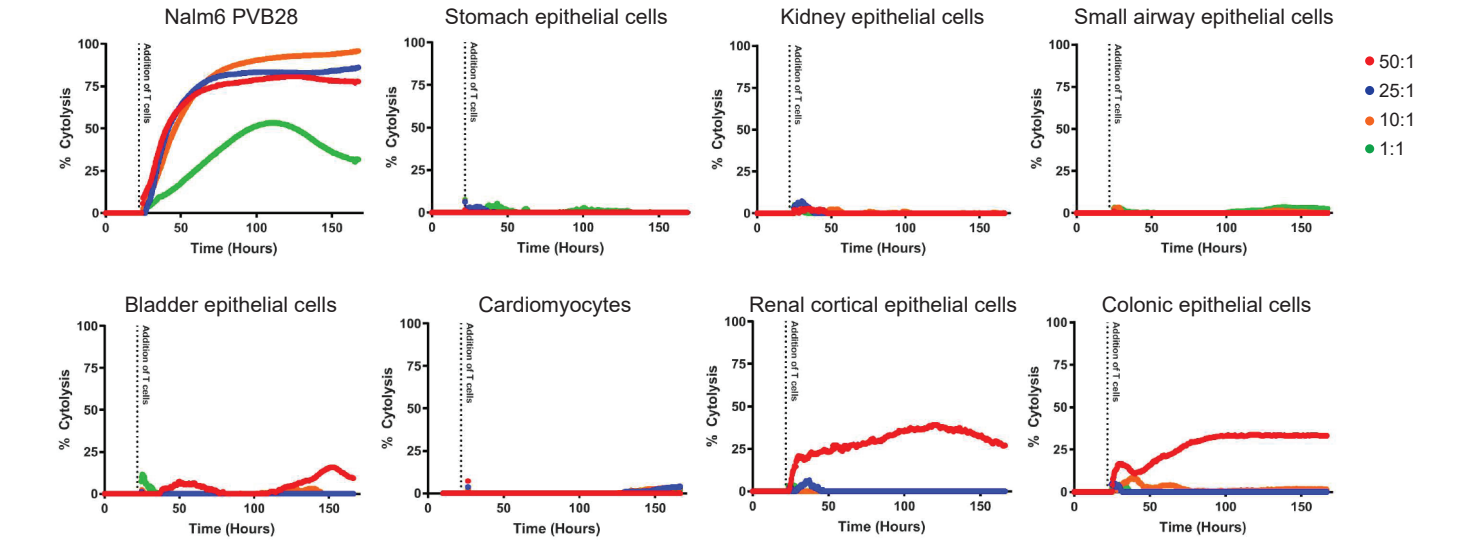

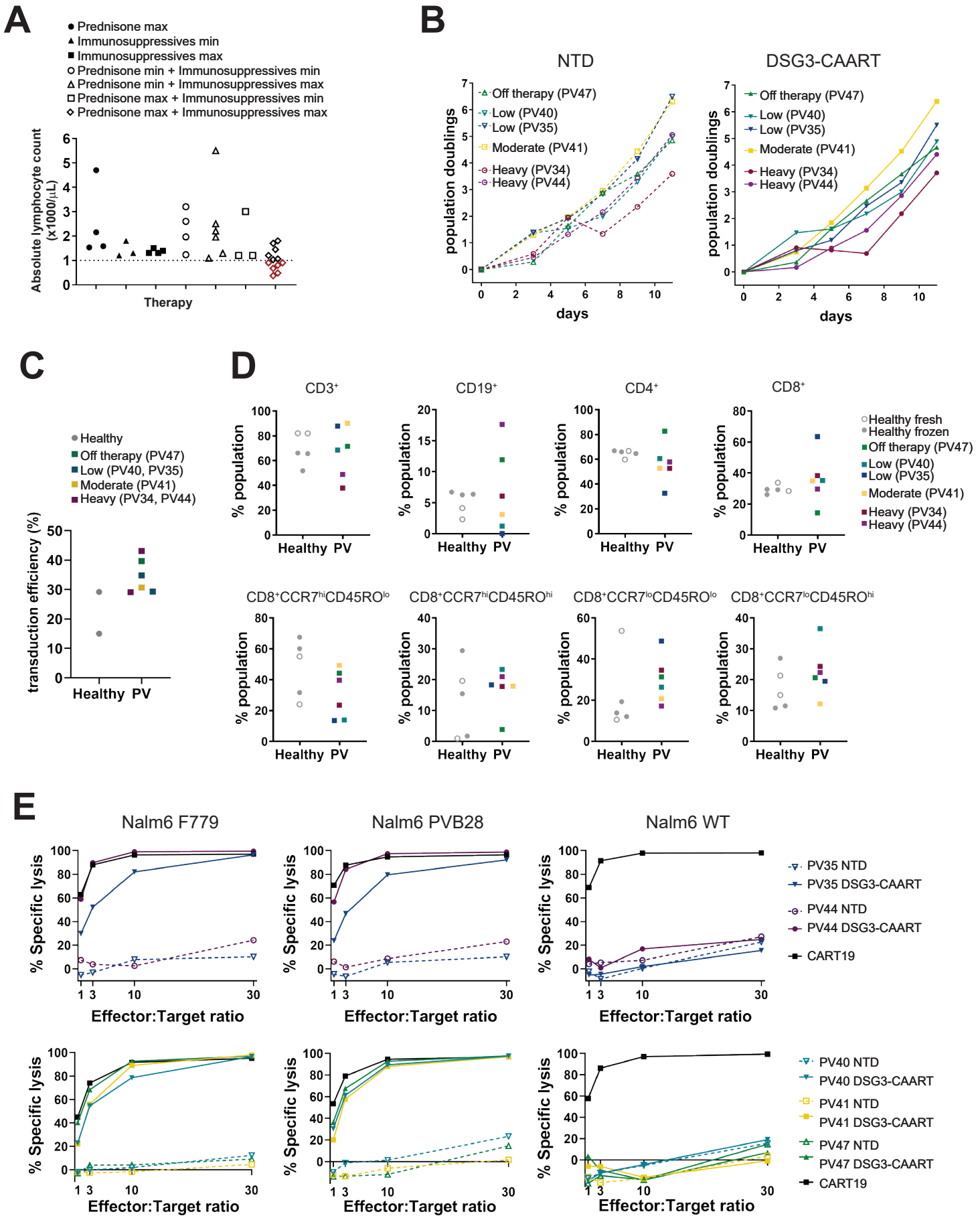

Supplementary Figure 8. DSG3-CAART cell manufacturing from PV patient T cells. (A) Absolute lymphocyte count in pemphigus patients receiving minimal (min) to maximal (max) doses of immunosuppressives (defined in Methods) exceeds the 1000/μL threshold for manufacturing feasibility, with the exception of 6 PV patients on maximal combined immunosuppressive regimens (red diamonds). (B) A trend toward decreased proliferation of NTD and DSG3 CAAR-transduced T-cells isolated from PV patients on heavy immunosuppressive regimens was observed; insufficient cells were manufactured from PV34 to perform cytotoxicity assays. (C) DSG3 CAAR transduction efficiency (determined by flow cytometry) was similar for T-cells isolated from healthy donors or PV patients on various immunosuppressive regimens. (D) PBMC subsets from PV patients do not significantly differ from healthy donor PBMCs. (E) DSG3-CAART manufactured from PV patients on low, moderate, or heavy immunosuppressive regimens demonstrated specific cytolytic activity against anti-DSG3 (F779 or PVB28) BCR-expressing but not wild type Nalm6 target cells, evaluated by a luciferase-based assay at the indicated E:T ratios.

	Anti-DSG3 antibody	Total T cell dose	Disease control	Toxicity	Relation to 1st cohort dose (cells/mL)
Figure 2	yes	$3x10^7$ (CAAR)	yes	1 of 5 mice	500x-2500x higher
Figure 2	yes	$1x10^7$ (CAAR)	yes	0 of 5 mice	167x-833x higher
Figure 2	yes	$3x10^6$ (CAAR)	partial	0 of 5 mice	50x-250x higher
Figure 2	no	$3x10^7$ (CAAR)	NA-no target cells	0 of 5 mice	500x-2500x higher
Figure 2	no	$1x10^7$ (CAAR)	NA-no target cells	0 of 5 mice	167x-833x higher
Ellebrecht et al, Science 2016 (Fig. 3A-D)	yes	$1x10^7$ (CAAR*)	yes	0 of 6 mice	167x-833x higher
Ellebrecht et al, Science 2016 (Fig. 3E, F)	yes	$5x10^6$ (CAAR)	yes	0 of 6 mice	83x-417x higher
Ellebrecht et al, Science 2016 (Fig. S8)	no	$3\text{-}4x10^6$ (CAAR)	yes	0 of 29 mice	~50x-250x higher
Suppl. Figure 2B-D	yes	$1x10^7$ (CAAR)	yes	0 of 12 mice	167x-833x higher
Suppl. Figure 2B-D	yes	$1x10^7$ (CAAR*)	yes	0 of 8 mice	83x-417x higher

Supplementary Table 1. Summary of in vivo experiments relating DSG3-CAART dose, activity, and toxicity. First column indicates source of data; last column indicates relationship between the dose used in mouse studies compared to the planned first cohort dose in humans. *Total CAART cell dose comprised of $5x10^6$ DSG3EC1-3 and $5x10^6$ DSG3EC1-4 CAART.